RESEARCH PAPER

Formulation and Optimization of Punica Granatum L Fruit Extract Loaded Self Emulsifying System and Its Prospective Antioxidant Activity in Hela Cell Lines

Muruganantham V[1*], Jitul Adhikary[1] and Ranganathan K[2]

[1]*Department of Pharmaceutics, Vinayaka Missions College of Pharmacy, Vinayaka Missions Research Foundation (Deemed to be University), Sankari Main road, Salem- 636308, Tamil Nadu, India*
[2]*Department of Pharmaceutics, AVB College of Pharmacy, Coimbatore, Tamil Nadu, India*

Received: 28th Feb, 2026; Revised: 6th March 2026; Accepted: 7th April, 2026; Available Online: 20th April, 2026

ABSTRACT

The study presents the design and optimization of a self-nanoemulsifying drug delivery system (SNEDDS) for enhancing the solubility, stability, and antioxidant efficacy of pomegranate (POM) extract rich in punicalagin and ellagic acid. The optimized formulation (OF2) comprised oleic acid (7.53%), Tween 80 (75.3%), and a polyethylene glycol : ethanol mixture (1:1, 17.17%), incorporating POM extract (17.22%) at its solubility threshold. OF2 exhibited rapid self-emulsification (< 20 s), high optical transmittance (> 97 %), and thermodynamic stability, forming a homogeneous nanoemulsion upon aqueous dispersion.

In vitro release followed first-order kinetics (R^2 = 0.986–0.997) with non-Fickian diffusion (n ≈ 0.57), achieving 98.8 % cumulative release within 2 h. Dynamic light scattering (DLS) revealed a trimodal particle-size distribution (20.1 ± 2.1 nm, 128.1 ± 7.8 nm, 402.2 ± 10.3 nm), PDI = 0.22 ± 0.02, and Zeta potential of –31.4 ± 1.2 mV, confirming electrostatically stabilized nanoscale dispersion.

The antioxidant evaluation demonstrated potent free-radical scavenging activity, with an IC_{50} = 84.87 µg/mL in the DPPH assay, consistent with high redox potential of the encapsulated polyphenols. In HeLa cells, pre-treatment with OF2 reduced H_2O_2-induced ROS generation by ~41 % and restored cell viability from 47 % to 79 %, as confirmed by fluorescence and WST-1 assays.

Optimized formulation, OF2, exhibited controlled release, strong antioxidant capacity, and marked cytoprotective effects. The developed SNEDDS provides a robust, scalable nanocarrier platform for improving oral delivery and therapeutic performance of polyphenol-rich phytoconstituents.

Keywords: *Pomegranate, Self emulsifying drug delivery system, Lipid-based nanocarrier, Antioxidant Supplement.*

How to cite this article: Muruganantham V, Adhikary J, Ranganathan K, Formulation and Optimization of Punica Granatum L Fruit Extract Loaded Self Emulsifying System and Its Prospective Antioxidant Activity in Hela Cell Lines. Int J Drug Deliv Technol. 2026;16(5): 258-279. DOI: 10.25258/ijddt.16.5.30

Source of support: Nil.

Conflict of interest: None

INTRODUCTION

Redox balance underpins life, with regulated shifts driving signaling, and excess ROS from aerobic metabolism causing oxidative damage to DNA, proteins, lipids, and carbohydrates[1]. Its also worth noting that cellular equilibrium relies partly on ROS-driven signaling[2]

Reactive oxygen species (ROS) are formed via enzymatic actions (e.g., NADPH oxidase, xanthine oxidase, NOS) and nonenzymatic triggers like ionizing radiation or oxygen interactions. Key ROS include superoxide ($O_2^{\bullet -}$), hydroxyl radicals (OH•), hydrogen peroxide (H_2O_2), and nitric oxide (NO•). Endogenous sources include inflammation, cancer, aging, and stress; exogenous sources include pollutants, drugs, smoke, alcohol, and radiation.[3]

**Author for Correspondence: Muruganantham V*

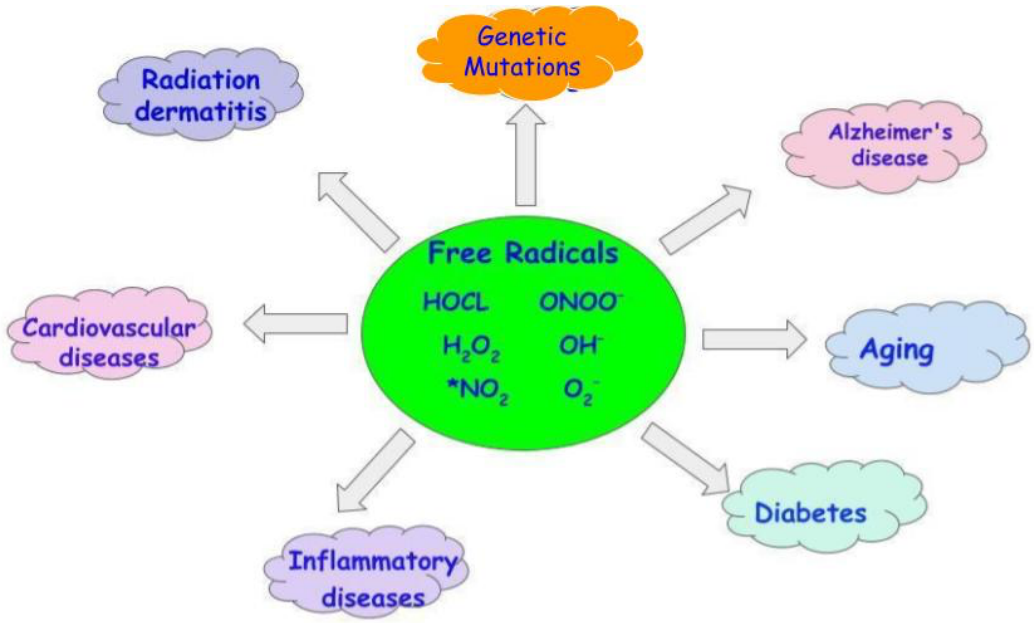

Figure 1 Free radicals linked to multiple pathological conditions

Oxidative stress occurs when oxidants overwhelm antioxidants, disrupting redox balance and causing molecular damage.[4] Elevated oxidative stress is associated with aging and various diseases, including cancer, neurodegeneration, cardiovascular and inflammatory disorders, diabetes, and substance abuse[5] During pregnancy, higher miscarriage rates are linked to ROS-detoxifying enzyme polymorphisms and selenium deficiency[2,6] Atherosclerosis results from oxidative stress–induced endothelial inflammation and macrophage-derived ROS production.[7] β-amyloid, a neurotoxic peptide generated by free radical activity, accumulates in Alzheimer's disease and contributes to its progression through oxidative neurodegeneration.[8]

Plant derived polyphenols are potent antioxidants that enhance and supplement the roles of antioxidant vitamins and enzymes.[9] Polyphenols are plant-derived compounds grouped into flavonoids, phenolic acids, stilbenes, and lignans. Phenolic acids are ubiquitous and make up about one-third of total polyphenols. Flavonoids, the most abundant in the diet, have two aromatic rings linked by three carbon atoms. Stilbenes and lignans feature distinct diphenolic structures formed through carbon bridging or dimerization. [10] For the current study *Punica granatum*(POM) fruit is selected. POM is native to northern India, Pakistan, Iran, pomegranates are also commonly grown in Africa, Arizona, California, Mexico, and Southwest America.. It has a lengthy history of ethnopharmacological application, including the possibility of immunological regulation, bactericidal, antifungal, and antiviral actions. Pomegranates can lessen the negative impacts of a number of ailments, including cancer, diabetes, and cardiovascular disorders as antioxidant. [11] The antioxidant activity of POM extract is due to the presence of vitamin C, B1, B2, and beta-carotene, major organic acids like tartaric acid, oxalic acid, malic acid, fumaric acid,, succinic acid and citric acid. The POM peel contains phenolic acid such as punicalagin, quercetin, and catechin, ellagic acid, caffeic acid, cinnamic acid, gallic acid, chlorogenic acid, pelletierine, hydroxy protocatechuic acid, hydroxy benzoic acid, ferulic acid, coumaric acid, isopelletierine, o-coumaric acid, methyl pelletierine, punicalin, pseudopelletierine, and glycoside flavonoids like Luteolin, kaempferol, and naringenin. Anthocyanin, a potent antioxidant, gives pomegranates their color. The red colour of the edible portions of POM fruit is caused by six anthocyanins, which are generated from pelargonidin, cyanidins, and delphinidins(also antioxidants). [12] Most of these compounds present in POM Extract belong to BCS Class 2/3/4 categories posing a significant problem in oral bioavailability and hence *in-vivo* antioxidant activity is minimal. Thus clinical benefit with antioxidant property is not achievable by oral delivery. Pre clinical data from *in-vitro* study shows a promising therapeutic effect but is limited by its bioavailability problem. [13]

The current study aims to improve oral bioavailability of POM fruit extract containing diverse antioxidant molecules such as ellagic acid, punicalin, punicalgin, gallic acid, Quercetin, and catechin etc. . This is achieved by formulating and optimizing a nano self-emulsifying delivery system loaded with POM extract. The bioavailability of POM extract can be improved by reducing the particle size and encapsulation of diverse individual constituents in POM extract in an O/W nanoemulsion system. This system can diffusion from within the GI tract while preventing hepatic first pass metabolism. Additionally lymphatic uptake can be promoted by use of long chain fatty acid as one of the components in formulation. POM extract designed in a Type IIIB LFCS formulation i.e. a Self nano emulsifying delivery system would theoretically work[14, 15,16]

In parallel, it is imperative to advance sustainable and environmentally responsible approaches in medicinal

development by employing the whole fruit as the raw material for extract preparation. Pomegranate (POM) is particularly well-suited for this purpose, as both its edible and inedible fractions are abundant in antioxidant bioactives. Notably, the edible arils constitute only ~40% of the total fruit weight, while the remaining ~60%—including peel, rind, and other by-products—is typically discarded. This practice not only results in the loss of valuable phytochemicals but also contributes substantially to agro-industrial waste. Valorization of these underutilized portions, coupled with strategies to minimize additional losses during production, supply chain management, processing, and retail, offers a dual benefit: maximizing the recovery of bioactive compounds while simultaneously reducing environmental burden.[17,18]

MATERIALS AND METHODS:

Materials

Analytical grade Aluminum chloride, Sodium Nitrite, Sodium hydroxide, sodium carbonate, methanol, ethanol were provided by the Department of Pharmaceutics, VMPC. Gallic acid was procured from Labogen, India. HeLa cell lines were procured from NCCS, Pune, India sourced by Capstone Biosciences, India. All other chemicals and reagents were of analytical grade and procured from Himedia and Sigma Aldich without further treatment.

Collection and Processing of plant material

The study involved the collection and authentication of POM fruits from Salem, Tamil Nadu, India, and its processing. The fruits were washed, peel and arils separated and freeze-dried. The seeds were then ground into a coarse powder using a mechanical grinder. The raw material was extracted by maceration for 72 hours, using ethanol as the solvent. Three batches of 20g crude raw material were defatted with petroleum ether for 24 hours, followed by extraction in 800ml of 80% ethanol. The resulting extract was dried using a vacuum evaporator and stored at 4 °C for further use.[19, 20]

Phytochemical Analysis

Wet-lab screening for the presence of ascorbic acid, carbohydrates, free amino acids, proteins, tannins, flavonoids, alkaloids, saponins, glycosides, steroids, and triterpenoids was carried out following the standard protocols described by Dubale *et al.* and Banu & Cathrine DL[21]

Estimation of Total phenolic content(TPC)

Folin Ciocalteu's technique was used to estimate the total phenolic content. Test tubes were filled with 1 ml of sample aliquots and gallic acid as standard (40µg/ml to1280µg/ml). This was followed by addition of 0.5 ml of Folin Ciocalteu's and 5 ml of distilled water and shaken and allowed to rest. At the Fifth minute, 2 ml of 20% sodium carbonate was added, and 10 ml of distilled water was added to the capacity followed by incubation at room temperature for 2 hours. After the emergence of deep blue colour, absorbance was determined using a UV visible spectrophotometer at 750 nm. Experiments were performed in triplicates. Total phenolic content was expressed as mg gallic acid equivalent/g POM extract(mgGAE/g POM extract)[22]

Estimation of Total flavonoid content(TFC)

Aluminum chloride colorimetric assay was used to determine the total flavonoid concentration. Test tubes were filled with 1 ml of sample and standard quercetin solution (40 to 1280 µg/ml aliquots were used), 3 ml distilled water, and half an ml of sodium nitrite solution(5%) and allowed to rest. At the 5th minute half an ml of 10% aluminum chloride was added and 2 ml of sodium hydroxide(1M) was introduced at the sixth minute. Ultimately, 10 ml of volume was created by adding distilled water and thoroughly mixing was done. The resulting yellowish-orange solutions were measured using a UV-visible instrument and gallic acid as standard, the absorbance was measured at 510 nm using a spectrophotometer. Distilled water was used for blank.[22]

Preformulation and optimization

Solubility studies

Screening of appropriate excipients is done by solubility studies.

The solubility of the pomegranate (POM) extract in selected oils, surfactants, and co-surfactants was evaluated in triplicate (n = 3) using a standardized equilibrium solubility method. Briefly, an excess amount of extract was dispersed in each vehicle, vortex-mixed at ambient temperature, and incubated at 37 °C for 48 h to achieve equilibrium. After centrifugation, the supernatants were filtered through a 0.45 µm membrane filter, and aliquots were diluted with 80% ethanol to ensure analytical compatibility. Solubility was determined by UV–Vis spectrophotometry at 750 nm using the Folin–Ciocalteu assay, and results were expressed as gallic acid equivalents (GAE). This method was selected to quantify phenolic constituents, the primary antioxidant bioactives in the extract. Among the tested systems, vehicles demonstrating the highest phenolic solubility were shortlisted for subsequent SEDDS formulation development, while excipients with known pharmacological activity were excluded to minimize biological interference.[21,22]

Although the Folin–Ciocalteu assay is known to potentially overestimate total phenolic content due to cross-reactivity with other reducing agents, it remains a robust and widely accepted screening tool for preliminary solubility assessment of complex plant extracts. The method offers high reproducibility, simplicity, and compatibility with multiple formulation excipients, making it particularly suitable for comparative solubility profiling in early formulation development.

Pseudoternary phase diagram

The oil phase, surfactant, and co-surfactant exhibiting the highest solubility of the POM extract were selected for microemulsion studies. Four systems were formulated to delineate the microemulsion region by varying the surfactant-to-co-surfactant (Smix) ratio and oil content,

using the aqueous titration method. The phase transition was monitored visually: a milky or opaque appearance indicated coarse emulsion formation, whereas a gradual change from turbid to transparent or colorless denoted the formation of a micro- or nanoemulsion. Based on these observations, pseudo-ternary phase diagrams were constructed to identify the compositional boundaries of the microemulsion region. The system exhibiting the largest and most stable microemulsion area was subsequently selected for optimized SEDDS formulation development.

ATR-FTIR Spectra analysis- Compatibility studies of chosen excipients

The wavelength range of 4000 cm-1 to 400 cm-1 was used to record the spectra. The IR spectra of extract, solvents and co-solvents and physical mixture were investigated using ATR-FTIR spectroscopy. [23]

Optimization using Box-Behnken design (Response surface method)

Based on the outcome pseudo ternary phase diagram, One of the systems was selected. The upper and lower limits of constraints were also identified. A four factor, three level design which needed 29 trial runs were performed. Design expert™ software was utilized for this purpose. The following four independent variables or components were taken into account: the amount of oil phase, the surfactant, the co-solvent, and the amount of POM extract; the response variables were transmittance and the self-emulsification time.

Formulation of self emulsifying drug delivery system(SEDDS)

Self-emulsifying systems are lipid-based formulations that spontaneously form fine oil-in-water emulsions upon mild agitation, such as that produced by gastrointestinal peristalsis. Based on the optimized pseudo-ternary phase diagram, formulations were prepared using 8–10% oil phase, 62–75% surfactant, and 7–9% co-surfactant, with the POM extract incorporated at 10–24% w/w of the total mixture. Initially, the extract was dissolved in the oil phase by vortex mixing, followed by the sequential addition of surfactant and co-surfactant with continuous mixing for 3 hours to ensure homogeneity. The mixture was then sonicated for 10 minutes in a bath sonicator to obtain a uniform dispersion. The prepared self-emulsifying drug delivery systems (SEDDS) were stored at ambient temperature for 24 hours prior to characterization to evaluate physical stability.

Characterization of SEDDS

Study of transmittance

Transmittance signifies the amount of light scattered, with smaller particle size, transmittance would be higher and vice versa. Study of transmittance was part of the formulation optimization. 1 ml of each of the SEDDS formulations as per the trial output form Design expert™ was diluted in 20 ml distilled water for recording the percentage transmittance while distilled water was used as a blank in a spectrophotometric measurement of percentage transmittance conducted in UV-Vis double beam spectrophotometry (Systronics UV-2202) at 650 nm.[24,25]

Drug loading efficiency of SEDDS

Drug loading efficiency (DLE) of the nano-SEDDS formulations was evaluated through total phenolic content (TPC), expressed in terms of gallic acid equivalents. For analysis, 1 g of each formulation was dispersed in 20 mL of distilled water, followed by the addition of 10 mL of ethanol, and centrifuged at 3000 rpm for 10 minutes. The resulting supernatant was filtered, and its TPC was quantified spectrophotometrically using gallic acid as the reference standard, as described earlier.[(28)] DLE was calculated as the percentage ratio of TPC (g gallic acid equivalent) to the weight of the formulation (g). [25]

Determination of pH

Measured using digital pH meter (Systronics pH system 362), pH of the formulation has effect on the dissolution time and absorption and stability of the formulation. The pH of API also has an effect on the stability and structural integrity of soft and hard gelatin capsules when SEDDS are filled into them.[26]

Determination of viscosity

Emulsions exhibit non-Newtonian flow characteristics. Viscosity of the SEDDS without dilution and 10X dilution were measured. A digital viscometer Safire model LMDV-100, spindle 1 and RPM 50 was used.[27,28]

Studies on thermodynamic stability

Since the drug's precipitation in an excipient matrix might negatively impact the formulation's performance, physical stability is crucial. Phase separation of the excipients due to inadequate physical stability of the formulation can impact both the medicinal effectiveness and bioavailability. The top six optimized formulations were subjected to *Cycle of heating and cooling.* A total of two cycles ranging from 4°C to 45°C in the refrigerator, with storage at each temperature for 24 hours. A centrifugation test was performed to see if SEDDS was stable at these temperatures.

Test of centrifugation

SEDDS that passed were centrifuged using a computerized centrifuge (Remi Motors Ltd.) at 3000 rpm for 20 minutes. In the event that SEDDS revealed no phase separation, a freeze-thaw stress test was conducted.

Cycle of freezing and thawing

For SEDDS, three freeze-thaw cycles between -21°C and +25°C were performed, with storage at each temperature for 24 hours. [29]

Determination of self-emulsification time

For the selected top six optimized formulations, A USP dissolution apparatus type II was used to determine self emulsification time. Each formulation(1g) added dropwise to 900 ml of 0.1N HCl at 37°C. Agitation with standard stainless steel dissolution paddle was done at 50 rpm to mimic peristaltic movement of the GI tract. Emulsification time was assessed visually.[29,30]

Robustness to Dilution

The study examined the robustness of SEDDS to dilution by dilution to 10 ml, 150 ml, and 900 ml using water, phosphate buffer pH 6.8, and 0.1 N HCl. After a 12-hour storage period, the diluted SEDDS were examined for indications of phase separation or drug precipitation.[31,32]

Determination of droplet size, zeta potential and polydispersity Index

For the finally selected optimized SEDDS, Zeta potential measurement was utilized to ascertain the charge of the droplets. Zeta potential aids in forecasting the stability and flocculation impact in emulsion systems. At some point, the zeta potential will drop below which the colloidal will coalesce because of attraction forces. A Zetasizer nano Ver. 8.02 was used to measure the droplet size and zeta potential, conductivity, viscosity and refractive index of the resulting emulsion. The studies are based on dynamic light scattering.[33,34]

In-Vitro Dissolution & release kinetics studies

In vitro experiments were performed by using a USP type 1 apparatus (rotating basket) cell with compartment capacity of 900 mL. 0.5 mL of prepared SEDDS formulation was filled in a hard gelatin capsule., and the dissolution compartment was filled with 900 mL 0.1 N HCl. The basket continually swirled at 50 rpm, and the temperature was maintained at 37°C. The samples were taken at various intervals up to 4 hours and examined for a percentage of drug release from the SEDDS by using a UV spectrophotometer at 750 nm by method described in estimation of total phenolic content(TPC) [35]

Invitro DPPH scavenging activity for Optimized SEDDS formulation.

The POM extracts' and Optimized formulations' capacity to scavenge DPPH was tested. 1 ml of 100 mM, pH 7.4 tris HCl buffer was combined with a 0.2 ml ethanol solution containing POM extracts at varying concentration (50–200 µg/ml). To the combination mentioned above, one ml 500 mM in 1.0 ml ethanol of 2,2-Diphenyl-1-Picrylhydrazyl solution was added. After giving the mixture a good shake, it was allowed to sit at room temperature for half an hour. The resultant solution's absorbance was measured using a UV-visible spectrophotometer set at 517 nm. Each experiment was run three times. Ethanol(80% v/v) (0.2 ml) was used as a blank, and 1.0 ml of DPPH ethanolic solution (500 mM) was utilized as the control. Ascorbic acid was used as positive control. [36]

ROS fluorescence imaging assay on HeLa cell line

HeLa cells were cultured in Dulbecco's Modified Eagle Medium (DMEM) supplemented with 10% fetal bovine serum (FBS) and 1% penicillin-streptomycin until confluence. The cells were harvested by trypsinization, pooled into a 15 mL conical tube, and resuspended in fresh medium before being seeded into 96-well tissue culture plates at a density of 1×10^5 cells/mL. After a 24-hour incubation at 37°C in a humidified 5% CO_2 atmosphere to allow adherence and recovery, the cells were washed with serum-free DMEM and treated with 84.87 µg/mL of the optimized self-emulsifying drug delivery system (SEDDS) formulation, OF2. Following another 24-hour incubation, the wells were washed with 1× PBS, and 100 µL of a 10 µM DCFH-DA working solution prepared in serum-free DMEM was added to each well. The plates were gently mixed and incubated at 37°C for 60 minutes to allow intracellular probe loading. Oxidative stress was then induced by treating the cells with 100 µM hydrogen peroxide (H_2O_2) prepared from a 30% stock solution, excluding the untreated control wells. Reactive oxygen species (ROS) generation was immediately examined using a ZOE Fluorescent Cell Imager (Bio-Rad) at excitation/emission wavelengths of approximately 495/520 nm (FITC channel), and fluorescence intensity was quantified to assess relative intracellular ROS levels among the treatment groups.[37,38]

WST-1 Based Cell Viability Assay

Parallel to the ROS assay, HeLa cells were seeded in 96-well plates at 1×10^5 cells/mL and subjected to identical treatments: untreated control, 100 µM hydrogen peroxide, OF2 SEDDS alone, and a combination of OF2 SEDDS pre-treatment followed by hydrogen peroxide exposure. After treatment, 10 µL of WST-1 reagent(Sigma-Aldrich) was added to each well containing 100 µL of serum-free DMEM. Plates were incubated for 2-4 hours at 37°C to allow metabolically active cells to convert the tetrazolium salt into a water-soluble formazan dye. Absorbance was measured at 450 nm (reference wavelength 630 nm) using a microplate reader. Cell viability was calculated as a percentage relative to untreated controls, providing a quantitative assessment of cellular metabolic activity and survival following oxidative stress and treatment. [39]

Statistical analysis:

Libreoffice calc, Graphpad prismTM and Design expert™ were used for statistical analysis.

RESULT:

Phytochemical analysis:

Phytochemical screening of the extracts revealed that the extract prepared with 80% (v/v) ethanol contained ascorbic acid, carbohydrates, tannins, flavonoids, alkaloids, saponins, glycosides, steroids, and terpenoids. In contrast, the aqueous extract showed the presence of ascorbic acid, carbohydrates, flavonoids, saponins, and glycosides. The 80% ethanol extract was selected for further studies, as aqueous extracts are more susceptible to microbial contamination and are generally less efficient in extracting polyphenolic constituents.

ATR-FTIR compatibility studies

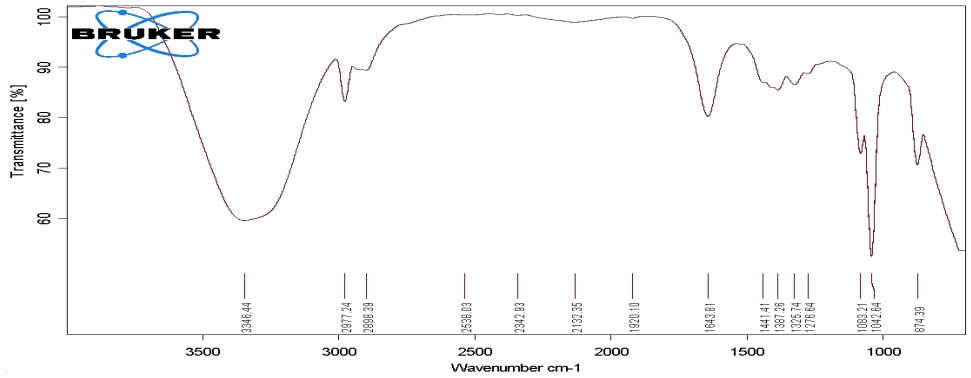

Figure 2 ATR-FTIR spectrum of *Pomegranate* extract dissolved in ethanol

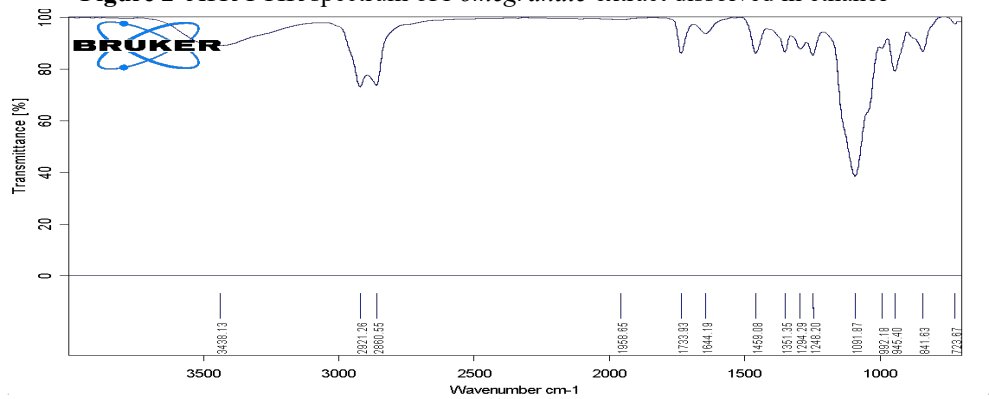

Figure 3 ATR- FTIR spectra of Tween 80 + Propylene Glycol + Oleic acid + Pomegranate Extract dissolved in Ethanol

The fingerprint region of the infrared spectrum (Figure 2 &3) exhibited characteristic peak transmittance at wavenumbers (cm^{-1}) 1441.41, 1387.26, 1325.74, 1276.64, 1083.21, 1042.64, and 874.39, corresponding to specific functional groups such as C–H bending (alkane), O–H bending (phenol, aldehyde, alcohol groups), C–N/C–O stretching (aromatic amine/aromatic ester, amine/primary alcohol groups), S=O or C–F stretching (sulfoxide or fluoro compounds), and C–H bending in 1,2,4-trisubstituted aromatic groups. Comparison of spectra from individual components and their physical mixture (Figure 1, & 2) revealed no significant shifts or new peaks, indicating the absence of chemical interactions and confirming compatibility among the components.[40,41]

Total Phenolic Content (TPC)

The total phenolic content (TPC) of the POM extract was found to be 251.33 ± 0.23 mg gallic acid equivalents (GAE) per gram of extract, as determined by the Folin–Ciocalteu method

Total flavonoid content (TFC)

The total flavonoid content (TFC) of the POM extract, determined using a quercetin standard calibration curve, was found to be 51.90 ± 0.62 mg quercetin equivalents (QE) per gram of extract.

Solubility studies

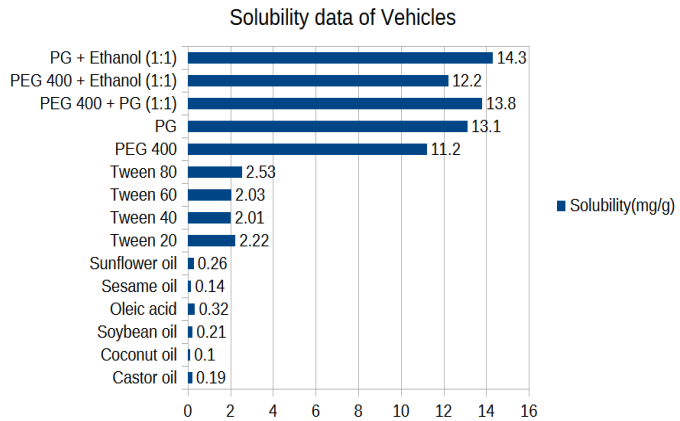

Figure 4 Solubility profile of phenolic compounds in various excipients. PG: Propylene Glycol; PEG: Polyethylene Glycol

Estimation of Total Dissolved Phenolic Content (TPC) for Solubility Profiling

The solubility of the POM extract in different formulation components was assessed(Figure 4) using total phenolic content (TPC) as a surrogate marker (Figure 4). The result is displayed as Mean ± SD (n=3). Since phenolic compounds represent the principal bioactive constituents, TPC was employed as an indirect measure of extract solubility. Among the oils examined, oleic acid showed the greatest solubilizing ability (0.32 ± 0.02 mg/g), which may be attributed to favorable lipophilic interactions and hydrogen bonding with polyphenolic moieties. In the case of surfactants, Tween 80 provided the highest solubility (2.53 ± 0.03 mg/g), consistent with its balanced hydrophilic–lipophilic properties and efficient emulsification capacity. The co-surfactant system of propylene glycol (PG) and ethanol (1:1) yielded the maximum solubility overall (14.3 ± 0.03 mg/g), likely due to synergistic co-solvency that enhances polarity and molecular diffusivity. Elevated solubility was also observed with PEG 400, PG, and PEG:ethanol mixtures. However, despite its high solubilizing potential, the PEG 400 + PG combination was excluded from subsequent formulation development because of its reported laxative effect and possible impact on oral tolerability

Pseudo ternary phase diagram

Based on the solubility studies, four systems were formulated (Table 1 & 2) and (Figure 5). Pseudo-ternary phase diagrams were constructed to identify the system exhibiting the largest microemulsion region for further optimization. Among the four systems, System 4, containing oleic acid, Tween 80, and propylene glycol (PG): Ethanol (1:1) as the oil, surfactant, and co-surfactant respectively, demonstrated the broadest microemulsion region. The endpoint of the titration was indicated by the appearance of turbidity upon further addition of distilled water. This observation suggests that the selected combination provided an optimal balance between interfacial tension reduction and surfactant–co-surfactant interaction, facilitating stable microemulsion formation.

Table 1 Systems for pseudo ternary diagram

System	Excipient 1	Excipient 2	Excipient 3
System 1	Oleic acid	Tween 80	Polyethylene glycol 400(PEG400)
System 2	Oleic acid	Tween 80	Propylene glycol(PG)
System 3	Oleic acid	Tween 80	PEG400 + Ethanol (1:1)
System 4	Oleic acid	Tween 80	PG + Ethanol (1:1)

Table 2 Proportions of Excipients for System 1,2,3 & 4

Formulation Number	Excipient 1(%)	Excipient 2(%)	Excipient 3(%)
1	70	15	15
2	65	15	20
3	65	20	15
4	50	35	15
5	50	45	5
6	25	70	5
7	20	70	10
8	10	80	10
9	10	82	8
10	10	83	7

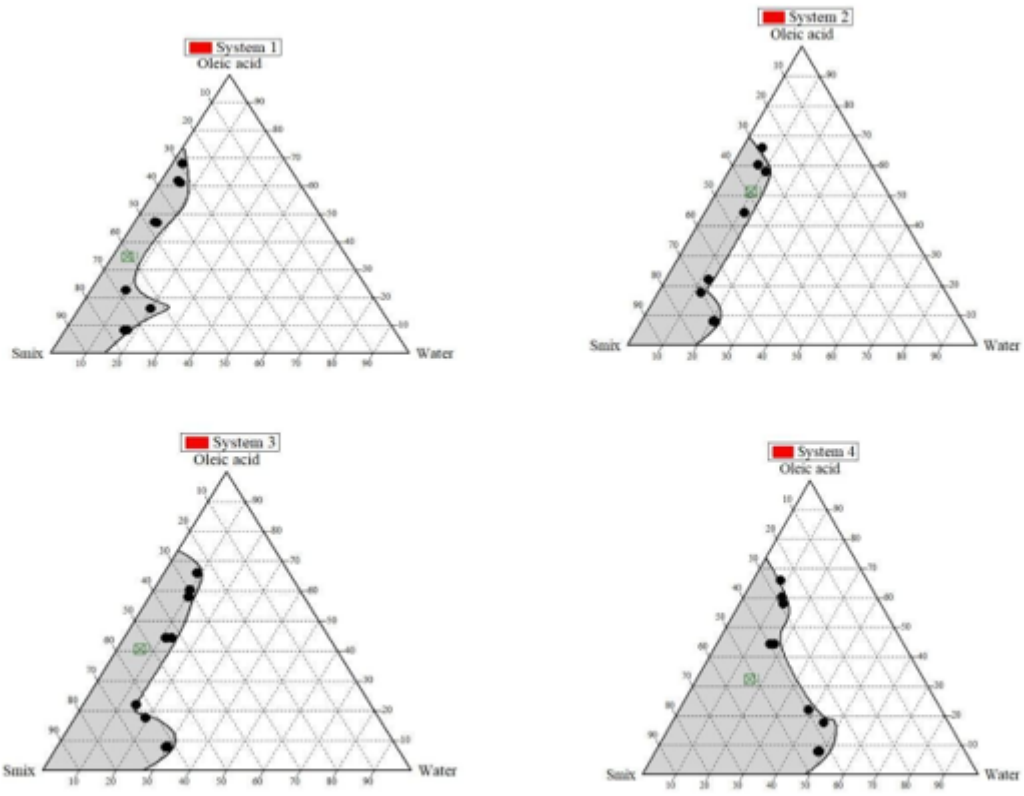

Figure- 5 Pseudo ternary phase diagram for systems 1 to 4, For details of system refer Tables 2 and 3

Optimization of Nano-SEDDS Using Box–Behnken Design

Based on the pseudo-ternary phase diagram, System 4, comprising oleic acid, Tween 80, and propylene glycol:ethanol (1:1), was selected for further optimization. A Box–Behnken response surface design (BBD) was employed to optimize the formulation variables. This design was chosen as it enables evaluation of the incremental cause–effect relationship between factors and responses, incorporates three center points for model reliability, and provides an efficient balance between experimental cost and predictive accuracy.

A total of 29 experimental runs were conducted based on the Box–Behnken design (Table 3, Figure 6) , and the data were analyzed using a quadratic ANOVA model for transmittance (Y_1). The ANOVA results (Table 4) indicated that the quadratic model was statistically significant ($F = 30.998$, $p < 0.0001$), confirming a strong correlation between the independent variables and the response. Among the individual factors, extract concentration (D) exhibited the most pronounced effect ($F = 320.423$, $p < 0.0001$), followed by oleic acid (A), Tween 80 (B), and PG:Ethanol ratio (C), all showing significant contributions ($p < 0.05$). Significant two-factor interactions were observed between A–B, A–C, and B–C, indicating synergistic effects among the oil, surfactant, and co-surfactant phases on transmittance. Quadratic terms A^2, C^2, and D^2 were also significant, suggesting curvature effects in the response surface. The model demonstrated an excellent fit ($R^2 = 0.9687$, Adjusted $R^2 = 0.9375$, Predicted $R^2 = 0.8396$), with a non-significant lack-of-fit value ($p = 0.2224$*), confirming that the model adequately represented the experimental data and possessed high predictive accuracy for transmittance optimization. Here A = Oleic acid, B = Tween 80, C = PG:Ethanol (1:1), D = POM Extract concentration.

Table 3 ANOVA for response- Transmittance (Y1)

Transmittance						
Quadratic Model- ANOVA						
Parameter	Squares sums	Degree of Freedom	Mean of Square	F Value	p-value, Prob > F	
Model	1,907.432	14	136.245	30.998	< 0.0001	significant
A-Oleic acid	75.000	1	75.000	17.064	0.001	
B-Tween 80	56.333	1	56.333	12.817	0.003	
C-PropyleneGlycol+Ethanol(1:1)	48.000	1	48.000	10.921	0.005	
D-POM Extract	1,408.333	1	1,408.333	320.423	< 0.0001	

AB	25.000	1	25.000	5.688	0.032	
AC	25.000	1	25.000	5.688	0.032	
AD	1.000	1	1.000	0.228	0.641	
BC	25.000	1	25.000	5.688	0.032	
BD	1.000	1	1.000	0.228	0.641	
CD	0.000	1	0.000	0.000	1.000	
A^2	21.016	1	21.016	4.782	0.046	
B^2	15.584	1	15.584	3.546	0.081	
C^2	21.016	1	21.016	4.782	0.046	
D^2	237.422	1	237.422	54.018	< 0.0001	
Residual	61.533	14	4.395			
Lack of Fit	52.333	10	5.233	2.275	0.2224	not significant
Pure Error	9.200	4	2.300			
Cor Total	1,968.966	28				

Derived Equation explaining Transmittance(Y1):

Transmittance (Y1) = 79.40 - 2.50A + 2.17 B - 2.00 C - 10.83 D - 2.50AB + 2.50AC - 0.50AD - 2.50BC + 0.50BD + 0.000CD + $1.80A^2$ +$1.55B^2$ + $1.80C^2$ + $6.05D^2$ .The significant quadratic model and interaction effects indicate that optimized ratios of oil, surfactant, and co-surfactant enhance optical clarity of the formulation, with extract concentration exerting the strongest influence on transmittance.

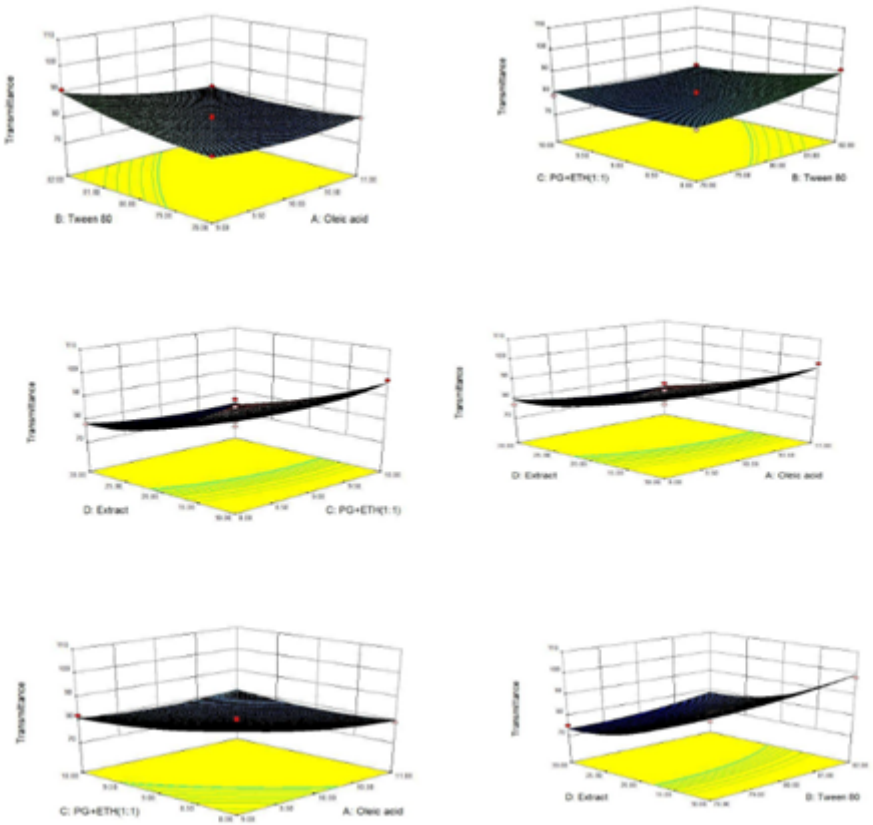

Figure 6 Response surface plots (Transmittance Y1)

From Figure- 5 Response surface curve of Transmittance, It was observed that an increase in Tween 80 while a corresponding decrease in Oleic acid increases transmittance. Similarly a decrease in oleic acid and a corresponding decrease in Propylene glycol: ethanol (1:1) increases transmittance. Higher transmittance was observed with lower quantity of POM extract(API) and oleic acid. An increase in Tween 80 and a decrease in [PG+Eth(1:1)] showed higher transmittance. An increase in tween 80 and decrease in extract also showed higher transmittance. Finally a decrease in both Propylene glycol: ethanol (1:1) and POM extract increased transmittance.

Selfemulsification Time:

Table 4 ANOVA for response- Emulsification time

Emulsification time						
Quadratic Model-ANOVA						
Parameter	Squares Sum	Degree of Freedom	Mean of Square	F Value	p-value, Prob > F	
Model	569.157	14	40.654	62.890	< 0.0001	significant
A-Oleic acid	44.083	1	44.083	68.195	< 0.0001	
B-Tween 80	16.333	1	16.333	25.267	0.0002	
C-PropyleneGlycol+Ethanol(1:1)	16.333	1	16.333	25.267	0.0002	
D- POM Extract	468.750	1	468.750	725.138	< 0.0001	
AB	1.000	1	1.000	1.547	0.2340	
AC	2.250	1	2.250	3.481	0.0832	
AD	1.000	1	1.000	1.547	0.2340	
BC	0.000	1	0.000	0.000	1.0000	
BD	0.000	1	0.000	0.000	1.0000	
CD	0.250	1	0.250	0.387	0.5440	
A^2	3.896	1	3.896	6.027	0.0278	
B^2	12.714	1	12.714	19.667	0.0006	
C^2	8.578	1	8.578	13.270	0.0027	
D^2	0.491	1	0.491	0.759	0.3984	
Residual	9.050	14	0.646			
Lack of Fit	8.250	10	0.825	4.125	0.0922	not significant
Pure Error	0.800	4	0.200			
Cor Total	578.207	28				

The ANOVA results (Table 4, Figure 7) demonstrated that the quadratic model for emulsification time was statistically significant ($F = 62.890$, $p < 0.0001$), confirming that the selected factors had a strong influence on the response. Among the individual variables, extract concentration (D) exhibited the most dominant effect ($F = 725.138$, $p < 0.0001$), followed by oleic acid (A), Tween 80 (B), and PG:Ethanol 1:1 ratio (C), each showing significant contributions ($p < 0.05$).

Quadratic terms A^2, B^2, and C^2 were also significant ($p < 0.05$), indicating curvature effects and nonlinearity in the response surface. In contrast, most interaction terms (AB, AC, AD, BC, BD, CD) were statistically insignificant ($p > 0.05$), suggesting that the factors primarily influenced emulsification time independently rather than synergistically.

The model displayed excellent fit statistics with $R^2 = 0.9844$, Adjusted $R^2 = 0.9689$, and Predicted $R^2 = 0.9125$, confirming its high predictive reliability. The lack-of-fit test ($p = 0.0922$) was non-significant, indicating that the quadratic model adequately described the experimental data.

Derived Equation explaining Self emulsification time(Y2):

Self emulsification time (Y2) = 18.20 + 1.92A - 1.17B + 1.17C + 6.25D + 0.50AB - 0.75AC - 0.50AD + 0.000BC + 0.000BD + 0.25CD + 0.78A2 + 1.40B2 + 1.15C2 + 0.27D2. The quadratic model revealed that higher surfactant and co-surfactant levels markedly reduced emulsification time, while increased oil and extract concentrations prolonged it, demonstrating their opposing effects on self-emulsification efficiency.

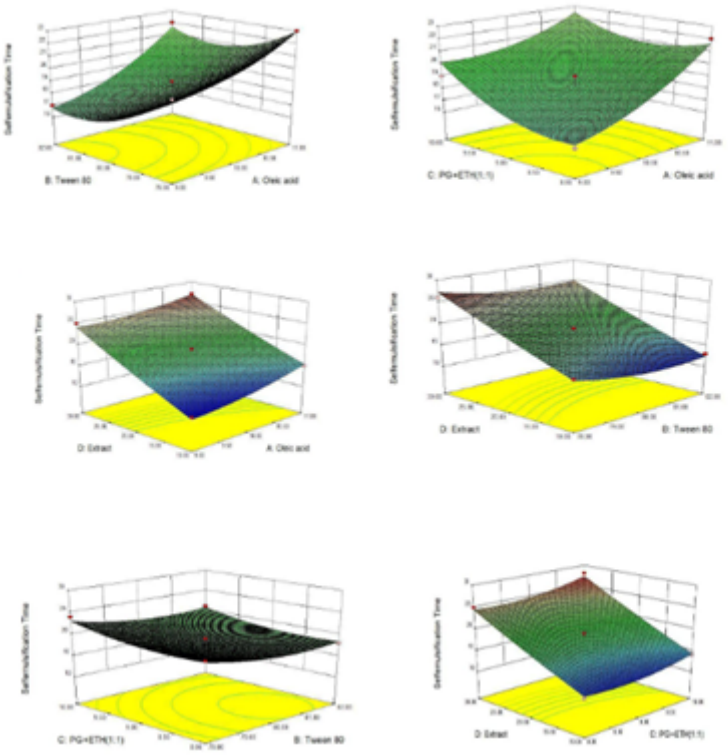

Figure 7 Response surface plots (Emulsification time Y2)

From the response surface curves(Figure- 6), It was observed that an increase in oleic acid and a decrease in Tween 80 increases self emulsification time, A decrease in both Oleic acid and Propylene glycol: ethanol (1:1) reduces self emulsification time. It was interesting to note that higher amounts of extract and corresponding higher amount of oleic acid increased self emulsification time. An increase in Tween 80 and a decrease in Propylene glycol: ethanol (1:1) decreases self emulsification time, it may be due to faster emulsion formation with one surfactant which is less stable. Cosurfactant form a much more stable emulsion. A reduced amount of Tween 80 and Exact also reduced self emulsification time. Similarly a reduced amount of Propylene glycol: ethanol (1:1) and extract decreased self emulsification time. The details are shown in Figure- 6

Output of Optimization

The six formulations (Table 6) exhibiting the highest overall desirability and most favorable predicted responses, as determined by the experimental design under the specified constraints (Table- 5), were prepared and evaluated for additional parameters. Table 7 presents the optimized formulations (OF1–OF6) along with their model-predicted values for transmittance and self-emulsification time.

Table 5 Constraints Applied for optimization

Variable	Goal	Lower Limit(%)	Upper Limit(%)
A: Oleic acid	Within set range	7	8
B: Tween 80	Within set range	61	74
C: PG+ETH (1:1)	Within set range	6	8
D: POM Extract	Within set range	10	25
Transmittance	Maximize	75	100
Self emulsification time	Minimize	11 seconds	28 seconds

Table 6 Optimized Formulations OF1 to OF6 selected with model predicted values of Design

Formulation code	**Oleic acid %**	**Tween 80 %**	**PG+Eth (1:1) %**	**Extract %**	**Transmittance (%)**	**Self Emulsification Time (sec)**	**Desirability**
OF1	7.54	68.67	6.7	17.1	98.31	16.3	0.7
OF2	7.53	68.57	6.69	17.22	98.16	16.41	0.7
OF3	7.56	68.85	6.72	16.88	98.62	16.09	0.7
OF4	7.5	68.31	6.66	17.53	97.76	16.7	0.7
OF5	7.49	68.21	6.65	17.65	97.6	16.82	0.7
OF6	7.58	69.09	6.74	16.59	99.02	15.83	0.7

Characterization of SEDDS:

Thermodynamic stability

All formulations pass the thermodynamic stability study. No formulation from OF1 to OF6 showed phase separation, turbidity or precipitation or color change at the end of thermodynamic stability test. It is significant as there remains flexibility on proportions for scale up if needed. All 6 SEDDS systems were subjected to characterization viz viscosity, pH and comparison of predicted vs wet lab self emulsification time & percentage Transmittance.

Viscosity

Viscosity of all the formulations OF1 to OF 6 was obtained, the formulation OF2 had the lowest viscosity of 64.4 ± 1.2 mpa.s. Lower viscosity is desirable as filling of SEDDS into hard or soft gelatin capsules becomes easier.

pH

The pH of formulations OF1-OF6 was in the range 5 to 6. Optimized formulation OF2 had a pH of 5.612 ± 0.212 in undiluted form.

Self- emulsification time and percentage transmittance for Optimized SEDDS

All the formulations OF1 to OF6 were subjected to transmittance study, the highest transmittance was observed for OF2 at 99.9 ± 0.01 % . Figure- 8 shows transmittance data.

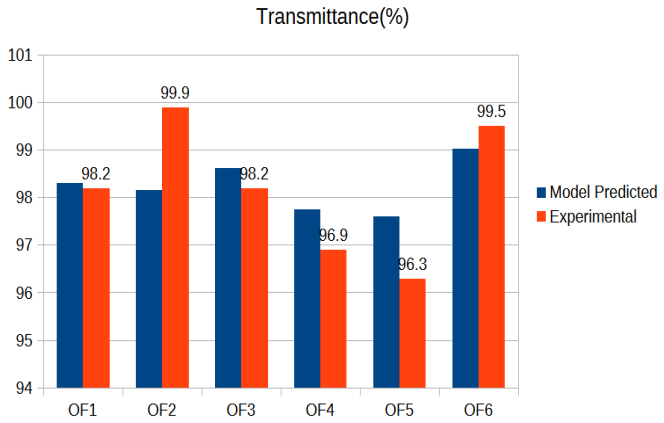

Figure 8 Transmittance of formulation OF1 to OF6 - Model predicted VS Experimental value

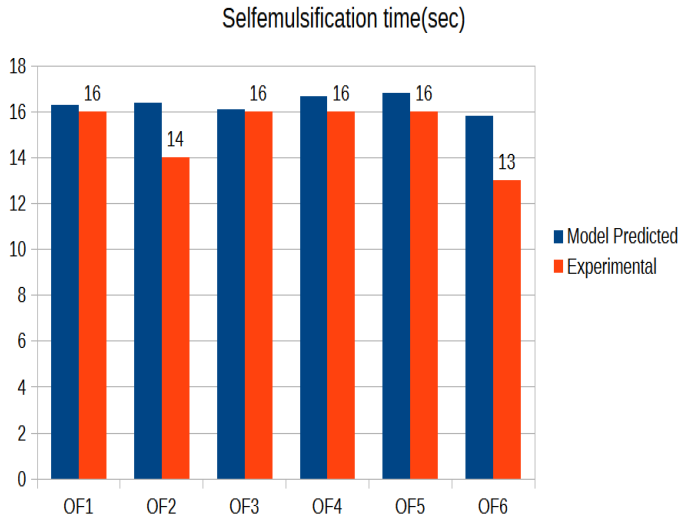

Figure 9 Self emulsification time of formulation OF1 to OF6 -Model predicted VS Experimental value

After the transmittance study all the formulations were tested for time required to self emulsify(Figure 9), it was compared with theoretical values from the experimental design. The lowest time taken to self emulsify was for OF6 at 13 ± 1.00 followed by OF2 at 14 ± 1.00 in seconds. All formulations self emulsified before 20 seconds. Figure- 10 is the graphical representation of self emulsification time of formulation OF1 to OF6.

Robustness to dilution and effect of pH

Robustness to dilution across different media is a critical indicator of emulsion stability under physiological conditions, as the gastrointestinal environment varies from acidic (stomach) to near-neutral or alkaline (intestine). All formulations (OF1–OF6) remained stable upon dilution with distilled water at volumes of 10 mL, 150 mL, and 900 mL, showing no signs of phase separation or turbidity. Similarly, the formulations exhibited excellent stability after 12 hours of storage in both 0.1 N HCl and phosphate

buffer pH 6.8 at the same dilution levels, without any evidence of precipitation or visual instability

Drug loading efficiency

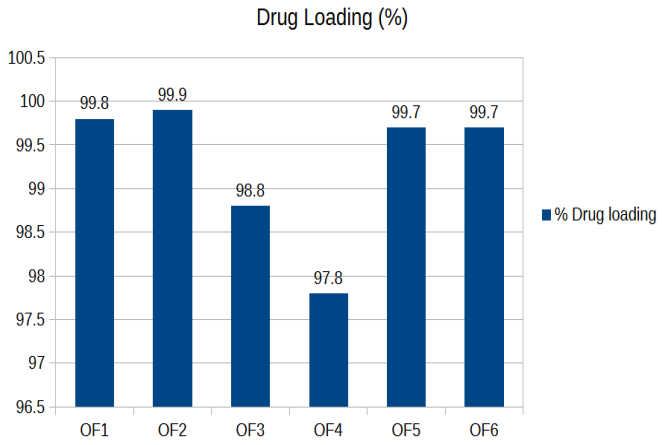

Figure 10 Drug loading efficiency of formulation OF1 to OF6

The formulation OF2 showed the maximum drug loading at 99.9%(Figure 10) and the lowest was shown by OF4 at 97.8% . Figure- 11, graphical representation of drug loading efficiency of formulation OF1 ton OF6.

In-vitro Dissolution studies & Release kinetics

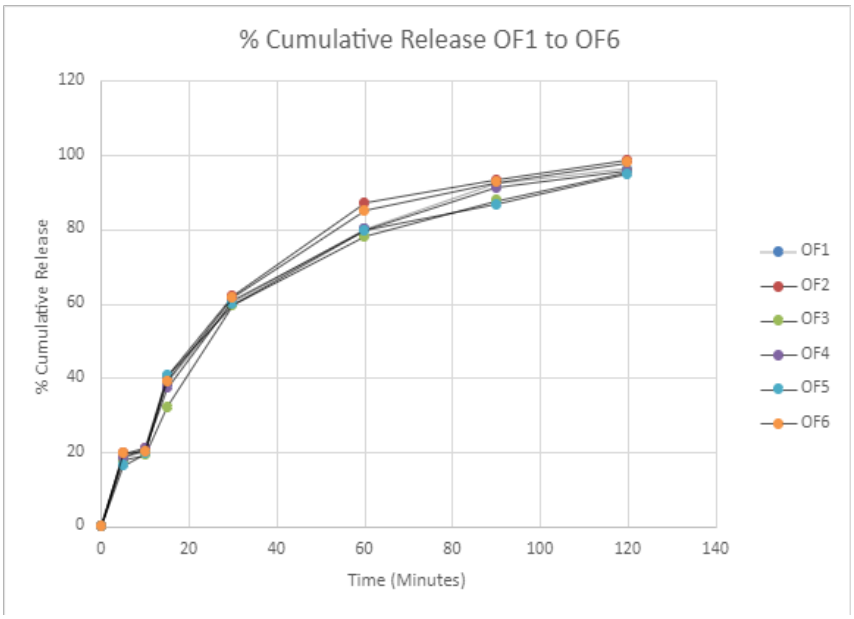

Figure 11 Percentage(%) cumulative drug release of formulation OF1 to OF6

Cumulative Drug Release Profile and Kinetic Evaluation

All formulations (OF1 to OF6) demonstrated rapid drug release, with percentage cumulative release exceeding 95% within the first 2 hours of dissolution testing (Figure 11 & Table 7)). Among these, formulation OF2 exhibited the highest release rate, achieving 98.82% cumulative drug release at the 2-hour mark. The kinetic release data for formulations OF1 through OF6 are summarized in Table 8, while the corresponding drug release profiles are graphically illustrated in Figure 12.

Table 7 *Kinetic modeling parameters of optimized SEDDS formulations (OF1–OF6).*

Formulation code	Zero order		First order		Higuchi		Hixson croswell		Korsmeyers Peppas	
	R^2	Slope	R^2	Slope	R^2	Slope	R^2	Slope	R^2	Slope
OF1	0.864	46.311	0.997	-0.712	0.97	74.395	0.975	-1.553	0.947	0.577
OF2	0.848	47.318	0.986	-0.913	0.962	76.437	0.979	-1.764	0.941	0.563
OF3	0.876	45.916	0.993	-0.652	0.971	73.312	0.978	-1.47	0.953	0.588

OF4	0.861	45.833	0.997	-0.684	0.969	73.76	0.973	-1.514	0.951	0.565
OF5	0.852	44.861	0.989	-0.625	0.964	72.377	0.966	-1.42	0.938	0.585
OF6	0.853	47.031	0.993	-0.829	0.964	75.815	0.978	-1.683	0.939	0.566

In Vitro Drug Release and Kinetic Modeling of Optimized SEDDS Formulations

The in vitro release profiles of the optimized self-emulsifying drug delivery systems (SEDDS) exhibited sustained-release behavior best described by first-order kinetics, with high correlation coefficients (R^2 = 0.986–0.997), indicating concentration-dependent release. The Korsmeyer–Peppas model yielded diffusional exponents (n = 0.563–0.588), confirming a non-Fickian (anomalous) transport mechanism governed by both diffusion and matrix relaxation. Among the evaluated formulations (OF1–OF6), OF2 showed the highest cumulative drug release (98.82% within 2 h) and was selected for further physicochemical characterization due to its superior release performance.

As summarized in Table 7, kinetic modeling revealed that while the Higuchi (R^2 = 0.962–0.971) and Hixson–Crowell (R^2 = 0.966–0.979) models showed moderate correlation, the first-order model consistently provided the best fit, confirming that the release rate decreased proportionally with drug concentration. The rapid self-emulsification (<20 s) and near-complete drug release (>95% within 2 h) suggest that the process is predominantly governed by emulsification-driven diffusion rather than simple matrix-controlled release. Overall, the results indicate that the optimized SEDDS formulations release the drug primarily through interfacial emulsification and diffusion mechanisms, with OF2 representing the most efficient system.

Particle size and zeta potential determination:

Table 8 DLS Particle Size Distribution — OF2 (n = 3)

Replicate	Peak 1 (nm)	Peak 2 (nm)	Peak 3 (nm)	% Below 30 nm	PDI	Zeta Potential (mV)	Interpretation
OF2R1	18.2	120.5	390.7	62%	0.21	–32.4	Stable colloid, good dispersion
OF2R2	22.4	135.8	410.3	59%	0.24	–30.1	Slight shift, acceptable
OF2R3	19.7	128.1	405.6	60%	0.22	–31.7	Consistent with OF2R1 and OF2R2

Dynamic light scattering (DLS) analysis(Table 8) of the optimized formulation (OF2) performed at 25 °C on a 25× diluted dispersion revealed a consistent trimodal particle size distribution, with mean peak diameters of 20.1 ± 2.1 nm, 128.1 ± 7.8 nm, and 402.2 ± 10.3 nm across three replicates (n = 3). The formulations exhibited PDI values between 0.21 and 0.24, indicating a relatively narrow size distribution within the dominant fraction. The zeta potential values (–30.1 to –32.4 mV) confirmed strong electrostatic stabilization and excellent colloidal stability under the measured conditions. Reproducibility across replicates indicated that the 25× dilution effectively minimized interparticle interactions without compromising the dispersion's stability, consistent with literature recommendations for optimal DLS analysis.

Considering that the major polyphenolic constituents of pomegranate extract—such as punicalagins (≈1.1 kDa) and ellagic acid (≈0.3 kDa)—possess molecular dimensions below 2 nm, the observed nanoscale populations can be attributed to their encapsulation within oil–surfactant aggregates formed during self-emulsification rather than the molecular size of the actives themselves. The smallest population (~20 nm) likely represents polyphenol-loaded micellar structures, whereas the 120–130 nm fraction corresponds to stable nanoemulsion droplets, and the 400 nm population reflects minor aggregates or transient coalescence. Although multiple size peaks appeared in the intensity plots, the relatively low PDI can be explained by the dominant scattering contribution of the mid-sized droplets, since DLS intensity scales with particle diameter (D^6).

From a formulation standpoint, these findings confirm that formulation OF2 forms a stable, self-dispersing nanosystem with efficient polyphenol encapsulation and reproducible electrokinetic stability, supporting its suitability for further oral delivery studies..[42,43,44,45]

DPPH free radical scavenging studies and calculation of IC50 Optimized formulation OF2

IC50 for Formulation OF2:

Table 9 Interpretation of Dose–Response Analysis for optimized Formulation OF2

Log of inhibitor vs. normalized response - with Variable slope	
Fit values	
LogIC50	1.929
HillSlope	2.262

IC50	84.87
Std. Error	
LogIC50	0.0314
Hill-Slope	0.3775
95% CI (asymptotic)	
LogIC50	1.861 to 1.997
HillSlope	3.078 to-1.447
IC50	72.60 to 99.22
Goodness of Fit	
Degrees of Freedom	13
R squared	0.9549
Sum of Squares	999.9
Sy.x	8.77
Number of points	
# of X values	15
# Y values analyzed	15

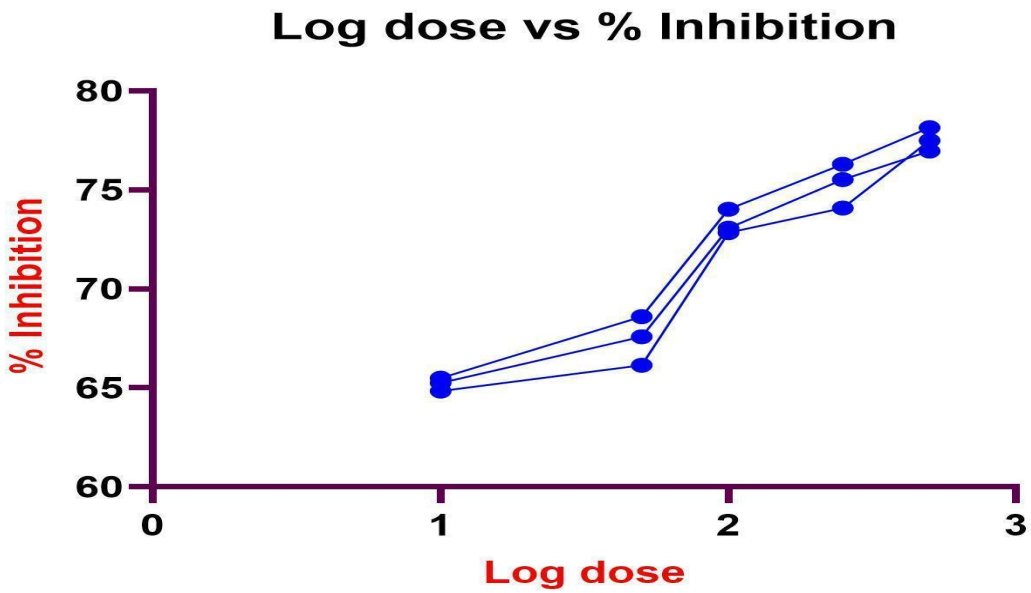

Figure 12 Log dose vs % inhibition of formulation OF2

The dose–response analysis(Table 9 & Figure 12) revealed that the inhibitor produced a half-maximal inhibitory concentration (IC_{50}) of 84.87 µM (95% CI: 72.6–99.2), corresponding to a $logIC_{50}$ of 1.929 ± 0.031, indicating moderate inhibitory potency. The Hill slope of 2.26 ± 0.38 suggests a relatively steep transition near the IC_{50}, implying potential cooperative binding behavior. However, the wide confidence interval (–1.45 to 3.08) indicates some variability and limits the precision of slope estimation. The nonlinear regression model exhibited an excellent fit (R^2 = 0.955) with a low residual standard deviation (Sy.x = 8.77) across 15 data points, confirming the reliability of the fitted curve. Overall, these findings demonstrate that the inhibitor exerts a concentration-dependent inhibitory effect with a well-defined IC_{50} and strong model conformity, though the slope parameter warrants cautious interpretation due to its variability.

Formulation OF2 was further evaluated for its qualitative in vitro reactive oxygen species (ROS) modulation potential using HeLa cell lines.

In vitro HeLa cell line ROS Qualitative assay

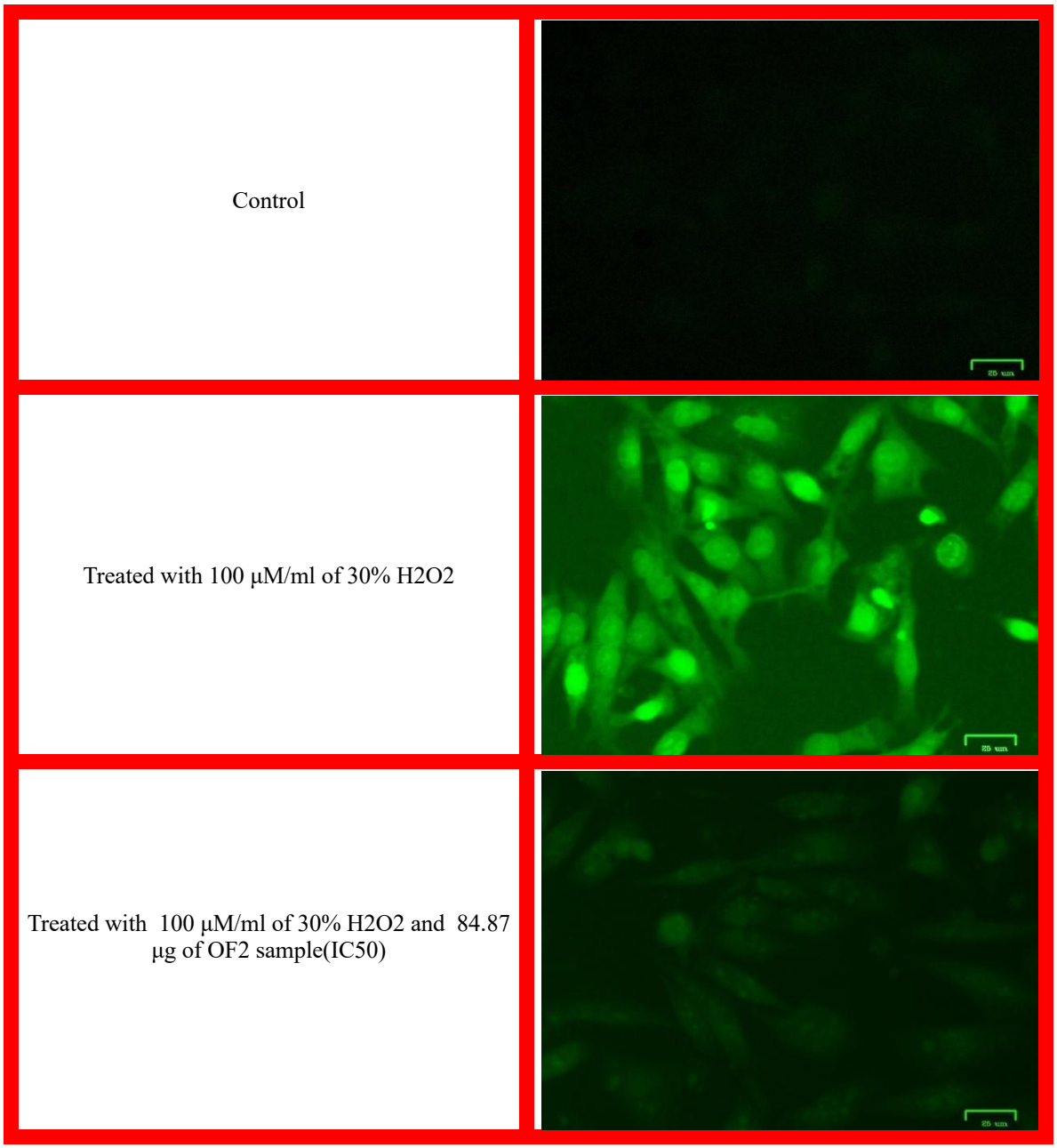

Figure 13 Influence of OF2 Pre-treatment on Fluorescence Intensity (ROS Levels) Under Oxidative Stress Conditions

Table 10 Effect of OF2 pre-treatment on H_2O_2-induced intracellular ROS levels measured by fluorescence intensity (RFU)

Group	Treatment	Fluorescence Intensity (RFU)	ROS Level Interpretation
Control	No treatment	489 ± 30	Baseline ROS (normal physiology)
H_2O_2	100 µM H_2O_2 only	1500 ± 50	High ROS due to oxidative stress
H_2O_2 + OF2	Pre-treatment with OF2, then 100 µM H_2O_2	880 ± 40	Moderate ROS, indicating significant inhibition

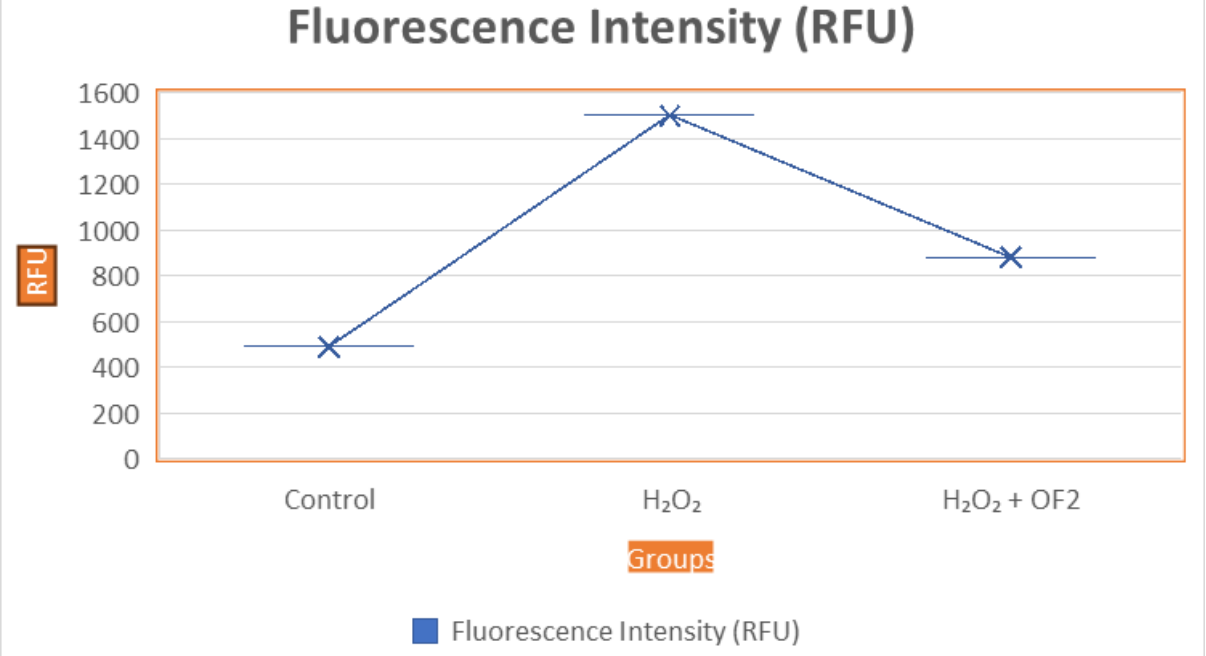

Figure 14 HeLa cell line ROS fluorescence assay

In HeLa cells(Table 10 & Figure 13), exposure to 100 µM hydrogen peroxide (H_2O_2) caused a pronounced elevation in intracellular reactive oxygen species (ROS), as reflected by a marked increase in fluorescence intensity (1500 ± 50 RFU; n = 3) compared with the untreated control (489 ± 30 RFU; n = 3), which represented basal physiological ROS levels. Pre-treatment with the optimized formulation (OF2) significantly mitigated this oxidative response, lowering fluorescence to 880 ± 40 RFU; n = 3, corresponding to approximately 41% inhibition relative to the H_2O_2-only group.

This attenuation of ROS generation indicates that OF2 exerts a pronounced cytoprotective effect against H_2O_2-induced oxidative stress, most likely through its phytoconstituents, including polyphenols and flavonoids, which are known free radical scavengers contributing to cellular redox homeostasis. Additionally, the self-emulsifying nanosystem may enhance intracellular delivery and bioavailability of these bioactives, thereby amplifying antioxidant potency. To verify that ROS suppression was not attributable to cytotoxic effects, a WST-1 assay was conducted in parallel to assess mitochondrial metabolic activity and overall cell viability, the results of which are described in the following section.[46,47,48]

Assessment of Cell Viability via WST-1 Assay

Assessment of Protective effect of OF2 on H_2O_2-induced oxidative stress and cytotoxicity in HeLa cells (Table 11). ROS levels were measured as fluorescence intensity (RFU), and cell viability was determined using the WST-1 assay. Pre-treatment with OF2 significantly reduced ROS generation (41% inhibition) and improved cell viability (79% relative to control) compared to H_2O_2-treated cells, indicating both antioxidant and cytoprotective effects. Data are presented as mean ± SD (n = 3).

Table 11 Protective effect of OF2 on H_2O_2-induced oxidative stress and cytotoxicity in HeLa cells.

Group	Treatment Description	ROS Fluorescence (RFU)	% ROS Inhibition	WST-1 Absorbance (450 nm)	% Viability	Interpretation
Control	No treatment	489 ± 30	–	0.90 ± 0.04	100%	Baseline ROS and cell viability
H_2O_2	100 µM H_2O_2 only	1500 ± 50	–	0.42 ± 0.03	47%	Elevated ROS and oxidative stress-induced cytotoxicity
H_2O_2 + OF2	Pre-treatment with OF2, then 100 µM H_2O_2	880 ± 40	41%	0.71 ± 0.03	79%	Significant ROS reduction and cytoprotection

A clear inverse correlation was observed between intracellular ROS levels and cell viability in HeLa cells

(Table X). Exposure to 100 μM H_2O_2 led to a pronounced increase in ROS fluorescence (1500 ± 50 RFU) with a concomitant decrease in WST-1 absorbance (0.42 ± 0.03 at 450 nm), indicating a reduction in metabolic activity to 47% viability. This confirms that excessive ROS generation induces oxidative stress–mediated cytotoxicity. In contrast, pre-treatment with the optimized formulation (OF2) significantly suppressed ROS levels to 880 ± 40 RFU (≈ 41% inhibition) while improving mitochondrial function, reflected by 79% viability (0.71 ± 0.03 absorbance).

These findings demonstrate that attenuation of ROS by OF2 is closely associated with improved cellular survival, supporting its cytoprotective potential under oxidative conditions. The data suggest that OF2's phytoconstituents, particularly polyphenols and flavonoids, may contribute to this effect through free-radical scavenging and mitochondrial protection. However, as these assays provide indirect measures of oxidative stress and viability, further mechanistic validation—such as mitochondrial membrane potential assessment, lipid peroxidation quantification, and apoptosis marker analysis—is warranted to confirm the precise pathways involved. Additionally, since the study employed a single cell line (HeLa) and limited biological replicates (n = 3), broader validation across different cellular models would strengthen the generalizability of these findings.

Collectively, the dual-parameter analysis establishes a strong inverse relationship between ROS accumulation and cell viability, underscoring the protective efficacy of OF2 against H_2O_2-induced oxidative injury in HeLa cells.

DISCUSSION

The optimized pomegranate extract–loaded self-nanoemulsifying drug delivery system (SNEDDS), designated formulation OF2, comprised oleic acid (7.53%) as the oil phase, Tween 80 (75.3%) as the surfactant, and a polyethylene glycol : ethanol mixture (1:1, 17.17%) as the co-surfactant, incorporating pomegranate (POM) extract (17.22%) at its solubility threshold. The pseudo-ternary phase diagram identified this composition as optimal, producing instantaneous self-emulsification (< 20 s) and high optical transmittance (> 97 %), indicative of a thermodynamically stable nanoemulsion. The rapid emulsification is attributed to a favorable interfacial free energy reduction and high surfactant curvature flexibility, which promotes spontaneous dispersion under mild agitation.

Response surface modeling demonstrated high predictive reliability (R^2 > 0.93) for both transmittance and emulsification time. Extract loading significantly affected droplet clarity, reflecting interfacial viscosity effects induced by adsorbed polyphenols, whereas elevated surfactant and co-surfactant ratios improved emulsification efficiency by minimizing interfacial tension. These effects align with Gibbs adsorption and Marangoni flow–driven mechanisms governing spontaneous emulsification.

Drug-release profiles of the optimized formulations (OF1–OF6) exhibited first-order kinetics (R^2 = 0.986–0.997) with non-Fickian diffusion (n = 0.56–0.59), indicative of a combined diffusion–erosion mechanism. Formulation OF2 achieved the highest cumulative release (98.8 % within 2 h), suggesting an optimal surfactant-to-oil balance that enhances interfacial transport without droplet coalescence.

Dynamic light scattering (DLS) analysis revealed a trimodal size distribution with intensity-weighted mean diameters of 20.1 ± 2.1 nm, 128.1 ± 7.8 nm, and 402.2 ± 10.3 nm, a PDI of 0.21–0.24, and a zeta potential of –31.4 ± 1.2 mV, indicating good colloidal stability. The size distribution reflects distinct populations corresponding to micellar aggregates, kinetically stable droplets, and minor coalescence events. The relatively low PDI arises from the dominant scattering intensity of mid-sized droplets, consistent with D^6 intensity scaling in DLS analysis.

The antioxidant potential of OF2 was further validated using the DPPH radical scavenging assay, which demonstrated a potent free-radical neutralizing capacity with an IC_{50} of 84.87 μg/mL (R^2 = 0.9549). This finding reflects efficient preservation of redox-active polyphenols during formulation and supports their enhanced functional accessibility within the nanosystem. The steep Hill slope (2.26 ± 0.38) indicates cooperative radical quenching behavior, likely facilitated by the dense interfacial arrangement of polyphenols within surfactant-rich domains. The strong correlation between in vitro antioxidant performance and DLS-stabilized nanoscale dispersion confirms that the formulation retains biological activity post-encapsulation.

In HeLa cells, OF2 pretreatment markedly suppressed H_2O_2-induced ROS fluorescence by ~41 % and restored cell viability from 47 % to 79 %, as assessed by WST-1 assay. The parallel improvement in redox status and mitochondrial activity demonstrates effective intracellular delivery and bioavailability of encapsulated polyphenols. Mechanistically, this effect is attributed to enhanced solubilization, membrane permeability, and intracellular retention, potentially through modulation of the Nrf2–Keap1 antioxidant response pathway.

However, certain limitations constrain direct translational interpretation. The in vitro release assay used static, non-lipolytic conditions, omitting the enzymatic and bile-mediated digestion processes of the gastrointestinal tract. Likewise, the HeLa model, though suitable for oxidative stress studies, does not mimic intestinal permeability or systemic pharmacokinetics. Furthermore, the use of ethanol as a co-surfactant may restrict long-term stability and industrial scalability.

To mitigate these challenges, future work should employ in vitro lipolysis–permeation coupling assays, Caco-2 or HT29-MTX intestinal models, and transition toward solid SNEDDS (S-SNEDDS) using adsorbents such as Aerosil® 200 or Neusilin® US2. These strategies would enhance thermodynamic stability, manufacturability, and translational predictability.

In summary, formulation OF2 demonstrated robust physicochemical stability, controlled release, potent free-radical scavenging activity (IC_{50} = 84.87 µg/mL), and significant cytoprotective effects against oxidative stress. Its optimized interfacial architecture and reproducible nanoscale characteristics position it as a promising oral nanocarrier for antioxidant phytoconstituents, though biopharmaceutical and toxicokinetic validation remains essential for clinical translation.

CONCLUSION

The optimized pomegranate extract–loaded self-nanoemulsifying drug delivery system (OF2)—composed of oleic acid (7.53%), Tween 80 (75.3%), polyethylene glycol : ethanol (1:1, 17.17%), and POM extract (17.22%)—successfully enhanced solubilization, dispersion stability, and biological efficacy of polyphenolic constituents. OF2 exhibited rapid self-emulsification (< 20 s), thermodynamic stability, and a nanoscale dispersion with a mean droplet diameter of ~128 nm (PDI ≈ 0.22; ζ = –31.4 mV). The system demonstrated first-order release kinetics (R^2 = 0.986–0.997) with non-Fickian diffusion (n ≈ 0.57), confirming diffusion–relaxation–controlled release behavior.

Functionally, OF2 displayed potent DPPH radical scavenging activity (IC_{50} = 84.87 µg/mL), indicative of preserved redox potential post-encapsulation. In HeLa cells, OF2 pretreatment mitigated H_2O_2-induced oxidative stress, reducing intracellular ROS by ~41% and restoring cell viability to 79%, validating its cytoprotective efficacy. The formulation's physicochemical robustness and consistent biological performance highlight its suitability as an oral nanocarrier for antioxidant phytoconstituents.

Future translation should include in vitro lipolysis–permeation coupling, intestinal co-culture permeability models, and solid SNEDDS transformation to improve stability, scalability, and regulatory compliance. Collectively, OF2 represents a mechanistically optimized, bioactive nanosystem capable of augmenting the oral delivery and therapeutic potential of polyphenol-rich extracts.

ABBREVIATIONS

POM: Pomegranate, BCS: Biopharmaceutical classification system, FTIR: Fourier transform infrared spectroscopy, ROS: Reactive oxygen species, SEDDS: Self emulsifying drug delivery system, TFC: Total flavonoid content, TPC: Total phenolic content.

CONFLICT OF INTEREST

The authors have no conflicts of interest regarding this investigation.

ACKNOWLEDGMENTS:

The authors would like to thank Vinayaka missions college of Pharmacy, Salem, Tamilnadu- a constituent college of Vinayaka Missions Research foundation (Deemed to be university) for providing the lab facilities.

REFERENCES

1. Sies, H., Berndt, C., & Jones, D. P. (2017). Oxidative stress. Annual Review of Biochemistry, 86(1), 715–748. https://doi.org/10.1146/annurev-biochem-061516-045037
2. Burton, G. J., & Jauniaux, E. (2011). Oxidative stress. Best Practice & Research Clinical Obstetrics & Gynaecology, 25(3), 287–299. https://doi.org/10.1016/j.bpobgyn.2010.10.016
3. Pizzino, G., Irrera, N., Cucinotta, M., Pallio, G., Mannino, F., Arcoraci, V., et al. (2017). Oxidative stress: Harms and benefits for human health. Oxidative Medicine and Cellular Longevity, 2017, Article 8416763. https://doi.org/10.1155/2017/8416763
4. Avery, S. V. (2011). Molecular targets of oxidative stress. Biochemical Journal, 434(2), 201–210. https://doi.org/10.1042/BJ20101695
5. Preiser, J. (2012). Oxidative stress. Journal of Parenteral and Enteral Nutrition, 36(2), 147–154. https://doi.org/10.1177/0148607111434963
6. Hussain, T., Murtaza, G., Metwally, E., Kalhoro, D. H., Kalhoro, M. S., Rahu, B. A., et al. (2021). The role of oxidative stress and antioxidant balance in pregnancy. Mediators of Inflammation, 2021, Article 9962860. https://doi.org/10.1155/2021/9962860
7. Ceriello, A. (2008). Possible role of oxidative stress in the pathogenesis of hypertension. Diabetes Care, 31(Suppl. 2), S181–S184. https://doi.org/10.2337/dc08-s245
8. Halliwell, B. (2001). Role of free radicals in the neurodegenerative diseases. Drugs & Aging, 18(9), 685–716. https://doi.org/10.2165/00002512-200118090-00004
9. Marchev, A. S., Yordanova, Z. P., & Georgiev, M. I. (2020). Green (cell) factories for advanced production of plant secondary metabolites. Critical Reviews in Biotechnology, 40(4), 443–458. https://doi.org/10.1080/07388551.2020.1731414
10. Pandey, K. B., & Rizvi, S. I. (2009). Plant polyphenols as dietary antioxidants in human health and disease. Oxidative Medicine and Cellular Longevity, 2(5), 270–278. https://doi.org/10.4161/oxim.2.5.9498
11. Abdollahzadeh, S., Mashouf, R. Y., Mortazavi, H., Moghaddam, M. H., Roozbahani, N., & Vahedi, M. (2011). Antibacterial and antifungal activities of Punica granatum peel extracts against oral pathogens. Journal of Dentistry, 8(1).

https://www.ncbi.nlm.nih.gov/pmc/articles/PMC3184731/

12. Shaygannia, E., Bahmani, M., Zamanzad, B., & Rafieian-Kopaei, M. (2015). A review study on Punica granatum L. Journal of Evidence-Based Complementary & Alternative Medicine, 21(3), 221–227. https://doi.org/10.1177/2156587215598039
13. Venusova, E., Kolesarova, A., Horky, P., & Slama, P. (2021). Physiological and immune functions of punicalagin. Nutrients, 13(7), 2150. https://doi.org/10.3390/nu13072150
14. Pouton, C. W. (2006). Formulation of poorly water-soluble drugs for oral administration: Physicochemical and physiological issues and the lipid formulation classification system. European Journal of Pharmaceutical Sciences, 29(3–4), 278–287. https://doi.org/10.1016/j.ejps.2006.04.016
15. Williams, H. D., Sassene, P., Kleberg, K., Calderone, M., Igonin, A., Jule, E., et al. (2014). Toward the establishment of standardized in vitro tests for lipid-based formulations, part 4: Proposing a new lipid formulation performance classification system. Journal of Pharmaceutical Sciences, 103(8), 2441–2455. https://doi.org/10.1002/jps.24067
16. Zhang, Z., Lu, Y., Qi, J., & Wu, W. (2021). An update on oral drug delivery via intestinal lymphatic transport. Acta Pharmaceutica Sinica B, 11(8), 2449–2468. https://doi.org/10.1016/j.apsb.2020.12.022
17. Coman, V., Teleky, B. E., Mitrea, L., Martău, G. A., Szabo, K., Călinoiu, L. F., et al. (2020). Bioactive potential of fruit and vegetable wastes. Advances in Food and Nutrition Research, 91, 157–225. https://doi.org/10.1016/bs.afnr.2019.07.001
18. Sreekumar, S., Sithul, H., Muraleedharan, P., Azeez, J. M., & Sreeharshan, S. (2014). Pomegranate fruit as a rich source of biologically active compounds. BioMed Research International, 2014, Article 686921. https://doi.org/10.1155/2014/686921
19. Mphahlele, R. R., Fawole, O. A., Mokwena, L. M., & Opara, U. L. (2015). Effect of extraction method on chemical, volatile composition and antioxidant properties of pomegranate juice. South African Journal of Botany, 103, 135–144. https://doi.org/10.1016/j.sajb.2015.09.015
20. Banu, K. S., & Cathrine, D. L. (2015). General techniques involved in phytochemical analysis. International Journal of Advanced Research in Chemical Science, 2(4), 25–32.
21. Molole, G. J., Gure, A., & Abdissa, N. (2022). Determination of total phenolic content and antioxidant activity of Commiphora mollis (Oliv.) Engl. resin. BMC Chemistry, 16(1). https://doi.org/10.1186/s13065-022-00841-x
22. Diem, Q. D. O., Angkawijaya, A. E., Tran-Nguyen, P. L., Huynh, L. H., Soetaredjo, F. E., & Ismadji, S. (2013). Effect of extraction solvent on total phenol content, total flavonoid content, and antioxidant activity of Limnophila aromatica. Journal of Food and Drug Analysis, 22(3), 296–302. https://doi.org/10.1016/j.jfda.2013.11.001
23. Diño, S. F., Edu, A. D., Francisco, R. G., Gutierrez, E., Crucis, P., Lapuz, A. M., et al. (2023). Drug-excipient compatibility testing of cilostazol using FTIR and DSC analysis. The Philippine Journal of Science, 152(6A). https://doi.org/10.56899/152.6a.08
24. Patel, D., & Sawant, K. K. (2007). Oral bioavailability enhancement of acyclovir by self-microemulsifying drug delivery systems (SMEDDS). Drug Development and Industrial Pharmacy, 33(12), 1318–1326. https://doi.org/10.1080/03639040701385527
25. Ghitman, J., Stan, R., Vlasceanu, G., Vasile, E., & Iovu, H. (2019). Predicting the drug loading efficiency into hybrid nanocarriers based on PLGA-vegetable oil using molecular dynamic simulation approach and Flory-Huggins theory. Journal of Drug Delivery Science and Technology, 53, 101203. https://doi.org/10.1016/j.jddst.2019.101203
26. Zilhadia, Z., Harahap, Y., Jaswir, I., & Anwar, E. (2022). Evaluation and characterization of hard-shell capsules formulated by using goatskin gelatin. Polymers, 14(20), 4416. https://doi.org/10.3390/polym14204416
27. Walters, K., & Jones, W. M. (2003). Measurement of viscosity. In Elsevier eBooks (pp. 45–52). https://doi.org/10.1016/B978-075067123-1/50006-5
28. Bhattad, A. (2023). Review on viscosity measurement: Devices, methods, and models. Journal of Thermal Analysis and Calorimetry, 148(14), 6527–6543. https://doi.org/10.1007/s10973-023-12214-0
29. Patel, P., Patel, H., Mehta, T., & Panchal, S. (2013). Self micro-emulsifying drug delivery system of tacrolimus: Formulation, in vitro evaluation and stability studies. International Journal of Pharmaceutical Investigation, 3(2), 95–102. https://doi.org/10.4103/2230-973X.114899
30. Singh, A. K., Chaurasiya, A., Singh, M., Upadhyay, S. C., Mukherjee, R., & Khar, R. K. (2008). Exemestane loaded self-microemulsifying drug delivery system (SMEDDS): Development and

optimization. AAPS PharmSciTech, 9(2), 628–634. https://doi.org/10.1208/s12249-008-9080-6

31. Agrawal, A. G., Kumar, A., & Gide, P. S. (2015). Self-emulsifying drug delivery system for enhanced solubility and dissolution of glipizide. Colloids and Surfaces B: Biointerfaces, 126, 553–560. https://doi.org/10.1016/j.colsurfb.2014.11.022
32. Ujhelyi, Z., Vecsernyés, M., Fehér, P., Kósa, D., Arany, P., & Nemes, D. (2018). Physico-chemical characterization of self-emulsifying drug delivery systems. Drug Discovery Today Technologies, 27, 81–86. https://doi.org/10.1016/j.ddtec.2018.06.005
33. Patel, P., Chaulang, G., Akolkotkar, A., Mutha, S., Hardikar, S., & Bhosale, A. (2008, December 28). Self-emulsifying drug delivery system: A review. Research Journal of Pharmacy and Technology. https://rjptonline.org/HTMLPaper.aspx?Journal=Research+Journal+of+Pharmacy+and+Technology%3bPID%3d2008-1-4-59
34. Ren, S., Mu, H., Alchaer, F., Chtatou, A., & Müllertz, A. (2012). Optimization of self-nanoemulsifying drug delivery system for poorly water-soluble drug using response surface methodology. Drug Development and Industrial Pharmacy, 39(5), 799–806. https://doi.org/10.3109/03639045.2012.710634
35. Li, H., Tan, Y., Yang, L., Gao, L., Wang, T., & Yang, X. (2014). Dissolution evaluation in vitro and bioavailability in vivo of self-microemulsifying drug delivery systems for pH-sensitive drug loratadine. Journal of Microencapsulation, 32(2), 175–180. https://doi.org/10.3109/02652048.2014.985340
36. Bhalodia, N. R., Acharya, R. N., & Shukla, V. J. (2011). Evaluation of in vitro antioxidant activity of hydroalcoholic seed extracts of Cassia fistula Linn. Free Radicals and Antioxidants, 1(1), 68–76. https://doi.org/10.5530/ax.2011.1.11
37. Murphy, M. P., Bayir, H., Belousov, V., et al. (2022). Guidelines for measuring reactive oxygen species and oxidative damage in cells and in vivo. Nature Metabolism, 4, 651–662. https://doi.org/10.1038/s42255-022-00591-z
38. Kumar, R., & Gullapalli, R. R. (2024). High throughput screening assessment of reactive oxygen species (ROS) generation using dihydroethidium (DHE) fluorescence dye. Journal of Visualized Experiments, 203, Article 66238. https://doi.org/10.3791/66238
39. Ngamwongsatit, P., Banada, P. P., Panbangred, W., & Bhunia, A. K. (2008). WST-1-based cell cytotoxicity assay as a substitute for MTT-based assay for rapid detection of toxigenic Bacillus species using CHO cell line. Journal of Microbiological Methods, 73(3), 211–215. https://doi.org/10.1016/j.mimet.2008.03.002 (pubmed.ncbi.nlm.nih.gov)
40. Valand, R., Tanna, S., Lawson, G., & Bengtström, L. (2019). A review of Fourier transform infrared (FTIR) spectroscopy used in food adulteration and authenticity investigations. Food Additives & Contaminants: Part A, 37(1), 19–38. https://doi.org/10.1080/19440049.2019.1675909
41. Rojek, B., & Wesolowski, M. (2018). FTIR and TG analyses coupled with factor analysis in a compatibility study of acetazolamide with excipients. Spectrochimica Acta Part A: Molecular and Biomolecular Spectroscopy, 208, 285–293. https://doi.org/10.1016/j.saa.2018.10.020
42. Bhattacharjee, S. (2016). DLS and zeta potential—What they are and what they are not? Journal of Controlled Release, 235, 337–351. https://doi.org/10.1016/j.jconrel.2016.06.017
43. Fischer, U. A., Carle, R., & Kammerer, D. R. (2011). Identification and quantification of phenolic compounds in pomegranate (Punica granatum L.) fruit and juice by HPLC–DAD–ESI/MS^n. Food Chemistry, 127(2), 807–821. https://doi.org/10.1016/j.foodchem.2010.12.156
44. Iravani, S. (2011). Green synthesis of metal nanoparticles using plants. Green Chemistry, 13(10), 2638–2650. https://doi.org/10.1039/C1GC15386B
45. Constantinides, P. P. (1995). Lipid microemulsions for improving drug dissolution and oral absorption: Physical and biopharmaceutical aspects. Pharmaceutical Research, 12(11), 1561–1572. https://doi.org/10.1023/A:1016268311867
46. Sun, C., Gui, Y., Hu, R., Chen, J., Wang, B., & Guo, Y. (2018). Preparation and pharmacokinetics evaluation of solid self-microemulsifying drug delivery system (S-SMEDDS) of osthole. AAPS PharmSciTech, 19(5), 2301–2310. https://doi.org/10.1208/s12249-018-1067-3
47. Sermkaew, N., & Plyduang, T. (2019). Self-microemulsifying drug delivery systems of Moringa oleifera extract for enhanced dissolution of kaempferol and quercetin. Acta Pharmaceutica, 70(1), 77–88. https://doi.org/10.2478/acph-2020-0012
48. Marrero-Morfa, D., Ibarra-Alvarado, C., Luna-Vázquez, F. J., Estévez, M., Ledesma, E. M., & Rojas-Molina, A. (2023). Self-microemulsifying

system of an ethanolic extract of Heliopsis longipes root for enhanced solubility and release of affinin. AAPS Open, 9(1). https://doi.org/10.1186/s41120-023-00086-5